Tensile Characterization of Ceramic Matrix Composites (CMCs) with Nondestructive Evaluation (NDE) Techniques

Jeongguk Kim* and Joon-Hyun Lee**

Key Words : Ceramic Matrix Composites (CMCs), Ultrasonic Testing, Infrared Thermography, Nondestructive Evaluation (NDE), and Tensile Testing

ABSTRACT

Two different types of nondestructive evaluation (NDE) techniques were employed to investigate the tensile behavior of ceramic matrix composites (CMCs). Two NDE methods, ultrasonic testing (UT) and infrared (IR) thermography, were used to assess defects and/or damage evolution before and during mechanical testing. Prior to tensile testing, a UT C-scan and a xenon flash method were performed to obtain initial defect information in light of UT C-scans and thermal diffusivity maps, respectively. An IR camera was used for in-situ monitoring of progressive damages. The IR camera measured temperature changes during tensile testing. This paper has presented the feasibility of using NDE techniques to interpret structural performance of CMCs.

1. Introduction

Continuous fiber reinforced ceramic matrix composites (CFCCs) are one of the promising materials for high-temperature structural applications [1]. CFCCs provide good corrosion and wear resistance, a balance of strength and toughness at higher temperature above 1,000°C, and they are lightweight, compared to metallic materials.

To encourage wide applications of CFCCs, nondestructi ve evaluation (NDE) of CFCCs is essential not only for a ssuring manufacturing quality and lifetime service applic ation, but also as a characterization means for the researc h and development of advanced materials. NDE techni ques, such as ultrasonic testing (UT) and infrared (I R) imaging, are powerful methods to investigate the fracture behavior and defect distribution in the comp osite.

However, relatively little work has been performed on relating the NDE techniques to the understanding of mechanical behavior of CFCCs. Therfore, the m ain objectives of the current research are to (1) apply N DE techniques to assure the quality and structural in tegrity of Nicalon™/SiC composites, (2) perform ND E using UT and IR thermography methods for the a nalyses of defect distributions that may affect mecha nical properties, (3) investigate tension behavior of Nicalon™/SiC composites with the aid of NDE meth ods, and (4) provide fracture and NDE information to aid in the fabrication, development, and selection of Nicalon™/SiC composites for structural applications.

* Research Institute of Mechanical Technology, Pusan National University, Busan, Korea.

** School of Mechanical Engineering, Pusan National University, Busan, Korea.

2. Experimental Procedures

2.1 The Materials Systems

Two different types of continuous Nicalon™ (Nippon Carbon Co. Ltd., Japan) fiber reinforced SiC CMCs were used for this study, i.e., plain-weave Nic alon™/SiC composites and 0°/90° cross-ply Nicalon ™/SiC composites. Nicalon™ is an amorphous/crystallite fiber, predominantly SiC, with a diameter of approximately 10 to 15 μm, and has a chemical composition of 59% Si, 31% C, and 10% O_2 by weight. Both composites have a fiber volume conte nt of 40%, and they were fabricated by the isotherm al chemical vapor infiltration (ICVI) technique [2].

2.2 NDE of Composites Before Mechanical Testing

Ultrasonic Testing (UT)

The ultrasonic NDE is the most widely used technique for the detection and characterization of composite materials [3-9]. UT is a nondestructive method in which beams of high-frequency sound waves are introduced into materials for the detection of both surface and internal flaws in the material [5-9]. In this research, ultrasonic amplitude measurements were performed using a through-transmission C-scan mode at a frequency of 15 MHz, in an immersion tank.

The reason for selecting the through-transmission ultrasonic (TTU) geometry is partly due to t

he high attenuation of the material and the difficulty of o btaining and interpreting pulse-echo signals. In the TTU approach, a time-gate is applied to encompass the transmitted signal and to record its amplitude during an UT C-scan. In this work, the transducers have a diameter of 1 .27 cm and a focus length of 5.08 cm.

The amplitude of the TTU signal is quite sensitive to the presence of internal defects, such as voids and delaminations, and to variations of the internal structure, such as the undulation of fiber tows. Any defects or internal material conditions that attenuate, scatter, or block the transmitting ultrasonic beam will result in a low TTU signal in the C-scan image.

Infrared (IR) Thermography

IR Thermography is a powerful NDE technique for the characterization of composite materials [10-12]. Since the composite materials show relatively high emissivities, composites are suited for examinations with or without surface treatments [10].

In this study, thermography was used to measure the thermal diffusivity. The current experimental system uses Parker's method [13] to calculate thermal diffusivity. Parker's method assumes no heat loss during the test. Although this assumption can generate a small systematic error (3-5%) in thermal diffusivity, this method was chosen because of its simplicity, and more importantly, because the main focus of the present research was on the variations from point to point. IR images were acquired using a PC, and thermal diffusivity was calculated pixel by pixel.

The theoretically predicted back-surface temperature, T, as a function of time, t, and specimen thickness, L, according to Parker [13] is given by

$$T(L,t)=\frac{Q}{\rho CL}\left[1+2\sum_{n=1}^{\infty}(-1)^n \exp\left(\frac{-n^2\pi^2}{L^2}\alpha t\right)\right] \qquad (1)$$

where Q is the radiant energy incident on the front surface, ρ is the density, C is the specific heat, L is the specimen thickness, and α is the thermal diffusivity. Thermal diffusivity is calculated using:

$$\alpha = 0.1388\, L^2/t_{0.5} \qquad (2)$$

where $t_{0.5}$ is the half-rise time [12,13].

2.3 Tensile Testing

Monotonic tensile tests were conducted using a computer-controlled Material Test System (MTS) 810 servohydraulic frame equipped with hydraulic grips. The tensile tests were performed at room temperature under displacement control at a cross-head speed of 0.5 mm per minute. In this study, dog-bone type flat specimens were used to investigate the damage evolution during the tests. The IR camera was employed for in-situ monitoring of the temperature change during the tests. Aluminum tabs were attached with epoxy glue at each side of the shoulder section of the coupon in order to avoid rupture of the grip parts during loading the sample.

3. Results and Discussion

Figure 1 presents the NDE results prior to mechanical testing, i.e., UT C-scans and thermal diffusivity maps for plain-weave and cross-ply Nicalon/SiC composites, respectively. UT C-scan results present a somewhat different aspect for plain-weave and cross-ply samples in terms of ultrasonic transmitted amplitudes. Plain-weave composite shows relatively higher values of a UT transmitted amplitude distribution through the overall gage section, while cross-ply sample presents generally lower values of UT transmitted amplitudes through the whole sample. Due to the attenuation and/or reflection of UT sound waves at the presence of pores and/or defects, relatively lower values of UT amplitudes have been obtained in the defects-contained areas. In this respect, cross-ply composite may contain more defects/pores than plain-weave sample. Generally, dark color areas indicate higher UT amplitude values and defect-free areas, while light color areas represent defects-contained regions.

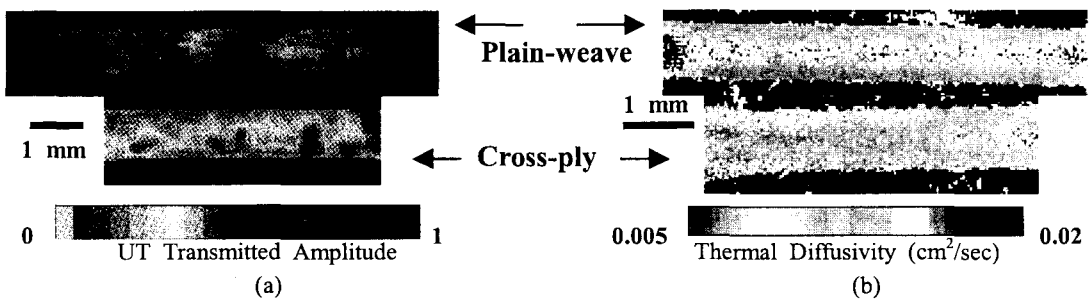

Fig. 1. A qualitative relation between (a) UT C-scans and (b) thermal diffusivity maps obtained for plain-weave and cross-ply Nicalon/SiC samples before mechanical testing, respectively. Note that all NDE results were obtai ned from the gage section of each dog-bone type flat bar tensile specimens.

In Fig. 1(a), cross-ply sample has a greater possibility to have defects in the composite than that of plain-weave sample. Figure 1(b) exhibits thermal diffusivity maps for plain-weave and cross-ply composites with a thermal diffusivity range of 0.005 to 0.02 cm^2/sec. A similar trend has been found in thermal diffusivity maps; plain-weave composite shows relatively higher thermal diffusivity values than cross-ply sample through the gage sections of the composites. Since the presence of defects retards the rate of the heat flow, relatively lower thermal diffusivity can be obtained in the areas around defects in cross-ply sample than plain-weave sample.

Seemingly, the qualitative consistency between the UT transmitted amplitude and thermal diffusivity has been presented in Fig. 1. In plain-weave composite, much higher thermal diffusivity can be seen along the centerline in the length direction of the sample, while cross-ply sample shows somewhat lower values of thermal diffusivity through the whole gage section of the specimen. Similarly, plain-weave sample demonstrates greater UT signatures than cross-ply sample. Qualitatively, an agreement between the two images of UT C-scans and thermal diffusivity maps seems to be present, i.e., very low values (dark color) of UT amplitudes can be seen on the left hand side of the gage section in cross-ply sample, and the corresponding area on the thermal diffusivity map [Fig. 1(b)] represents low values (light color) of thermal diffusivity. A qualitative agreement can be found in the comparison between the UT C-scans and thermal diffusivity maps, as shown in Figs. 1(a) and (b), i.e., plain-weave composite exhibits greater UT transmitted amplitudes and thermal diffusivity than cross-ply composite.

After the investigation of the qualitative correlation between the UT amplitude and thermal diffusivity, quantitative analyses have been conducted on Nicalon/SiC samples based on both NDE results. The current image analyses were performed on a Macintosh computer using the public domain NIH Image program [developed at the U.S. National Institutes of Health (NIH)] to establish a quantitative relationship between the UT amplitude and thermal diffusivity. Since both images, UT C-scan and thermal diffusivity images, presented more variations along the length direction of the specimen, a line profile was drawn along the length direction of the specimen. Also, the line was drawn at the center of the width direction of the specimen.

Figure 2 shows the relation between the UT amplitude and thermal diffusivity for plain-weave and cross-ply Nicalon/SiC composites, respectively. As predicted in previous images (Fig. 1), cross-ply sample presented relatively low values of thermal diffusivity and UT amplitude, compared to plain-weave sample. It is said that the UT amplitude increases as thermal diffusivity increases, as exhibited in Fig. 2, for both plain-weave and cross-ply composites. Overall, it was observed that the thermal diffusivity increases with increasing the UT amplitude as shown in Fig. 2.

Although the relationship between the two images of the UT C-scan and thermal diffusivity map seems to exist, it is difficult to say that whether it is linear, exponential, or polynominal function. Further study is needed to predict the exact trend between the two images.

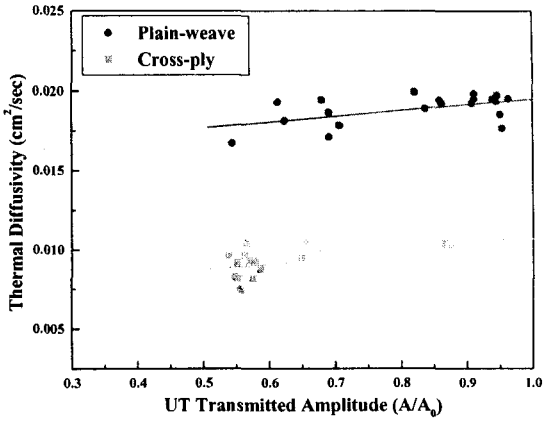

Fig. 2. Thermal diffusivity increasing with UT amplit ude for plain-weave and cross-ply Nicalon/SiC compo sites, respectively.

Figures 3 and 4 present IR camera images and temperature evolutions during tensile testing for plain-weave and cross-ply Nicalon/SiC composites, respectively. The temperature increase has been observed at the time of fracture. The IR camera speed was 2 Hz, which means that every half a second, the temperature evolution information was captured. The lower picture [Fig. 3(c)] shows the temperature evolution at the moment of fracture of plain-weave Nicalon/SiC composite, and the upper picture [Fig. 3(a)] presents the result at just half a second before failure.

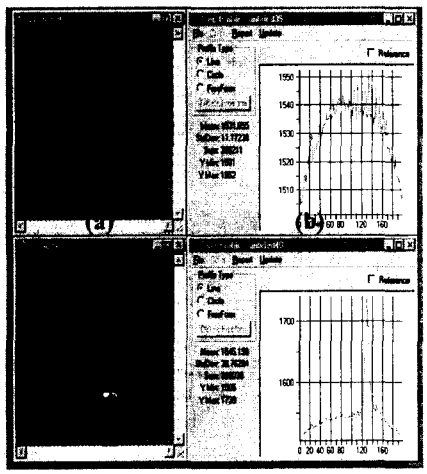

(c) (d)

Fig. 3. IR camera images and temperature evolution during tensile testing for plain-weave Nicalon/SiC composite.

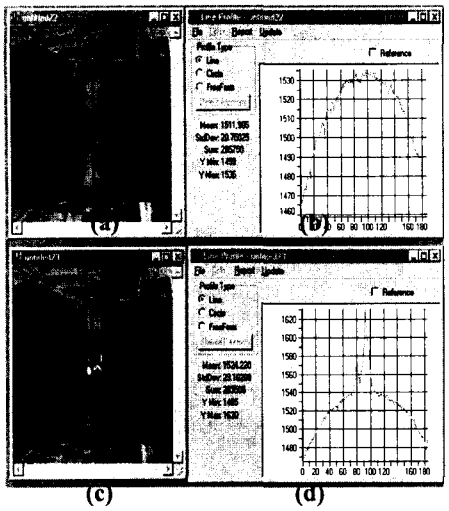

Fig. 4. IR camera images and temperature evolution during tensile testing for cross-ply Nicalon/SiC composite.

In order to display temperature variation along the length direction of the sample, a line profile was drawn as shown in Figs. 3(a) and (c) and Figs. 4(a) and (c). The right-hand side profiles, Figs. 3(b) and (d) and Figs. 4(b) and (d), represent the actual temperature increases before and at the moments of failures, respectively. Especially, Figs. 3(b) and 4(b) exhibit the hump shape temperature variations along the length direction of the sample. This is due to the heat conduction along the length direction (x-axis), i.e., there is heat conduction to both cold ends of the sample. As a result, the center of the sample has a greater temperature than both ends of the sample. Note that those data are still under careful investigations, and the plots in this paper are based on preliminary testing data. The temperature calibration results before and after tensile testing showed that a 30 IR unit represents 1K for both composites. The plots exhibit temperature variations along the length direction of the sample (x-axis) with the IR unit (y-axis) in Figs. 3 and 4. In Fig. 3, the plain-weave Nicalon/SiC composite shows the IR range of 1,505 to 1,739 unit. Therefore, we can infer that a temperature increase of about 8°C has been shown at the time of fracture [Fig. 3(d)].

Similar results have been obtained in the case of cross-ply composite as shown in Fig. 4. However, a lower temperature increases have been obtained as compared with plain-weave composite. The cross-ply Nicalon/SiC composite presents a temperature peak about 160 IR unit (about 5°C) at the moment of failure, as shown in Fig. 4(d).

Generally, plain-weave composite sample exhibited a higher temperature increase at the time of failure, while cross-ply composite sample presented lower temperature increases than plain-weave composite. This is mainly due to different fracture mechanisms of those composites. The temperature evolution at failure can be possible, resulting from frictional forces and interfacial debonding and sliding between the fiber and matrix. Although scanning electron microscopy (SEM) work is still required to investigate the fracture surface of tested sample, the composites had different fracture mechanisms, i.e., plain-weave composites showed matrix cracking and debonding at the fiber/matrix interface followed by fiber pullout through the whole layers of composite without delamination between each layer, and the failure occurred along the normal direction to the loading direction. On the contrary, in the case of cross-ply composites, the delaminations between the 0° and 90° laminae, parallel to the loading direction, occurred first, and fiber debonding and fiber pullout of each lamina was followed subsequently along the normal direction to the loading direction until final failure. At this point, we could infer that the layers of 2-dimensional composite architecture (plain-weave composite) provides stronger frictional forces between the fiber and matrix than the combination of delamination and single laminar fracture (cross-ply composite), which gives a greater temperature at fracture in plain-weave composite sample than cross-ply composite. Therefore, the difference in the amount of frictional forces of the composites resulted in different temperature increases.

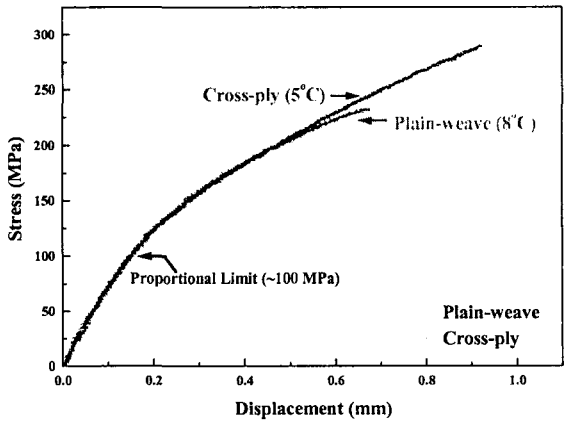

Fig. 5. The tensile stress-strain behavior of plain-weave and 0°/90° cross-ply Nicalon/SiC composites.

Figure 5 presents the tensile stress-strain behavior of plain-weave and cross-ply Nicalon/SiC composites. The numbers indicate the temperature increases at the time of failure measured from the IR camera investigation. In Fig. 5, the ultimate tensile strength (UTS) values are about 230 MPa for plain-weave composite, and 290 MPa for 0°/90° cross-ply composites, mainly due to the different fiber and laminate architecture. The tensile stress-strain behavior for both

composites exhibits very similar except showing different UTS values. After proportional limit (about 100 MPa), the stress-strain behavior of both composites shows plastic deformation-like behavior due to the subsequent fiber breakage and fiber pullout, and presents enhanced fracture toughness as compared with monolithic ceramics, which show only linear elastic behavior.

4. Conclusions

The current study provides the following summary.

1. Both qualitative and quantitative relations betwee n the UT transmitted amplitude and thermal diffusivi ty have been observed; qualitatively, an agreement between the UT C-scan images and thermal diffusivity maps has been presented, and quantitatively, thermal diffusivity increases as the UT amplitude increases in Nicalon/SiC composites.
2. There is an agreement between the NDE predicti ons and tensile testing results in assessing mechanica l properties of CMCs.
3. The combination of several NDE techniques can assure greater reliability for CMCs evaluation to inv estigate the fracture behavior of Nicalon/SiC compos ites.

Acknowledgments

This work is supported by the National Science Foundation. The authors would like to express great appreciation to Prof. Peter Liaw at the University of Tennessee, Knoxville, Tennessee, U.S.A. for his support and help on this investigation.

References

(1) R.L. Lehman, S.K. El-Rahaiby, and J.B. Wachtman, Handbook on Continuous Fiber-Reinforced Ceramic Matrix Composites,The Am. Ceram. Soc., p. 495 (1995).
(2) T.M. Besmann, B.W. Sheldon, R.A. Lowen, and D.P. Stinton, Science, 253 September, p. 1104, (1991).
(3) Nondestructive Testing Handbook, 2nd ed., vol. 10, Nondestructive Testing Overview, Stanley Ness, Charles N. Sherlock, technical editios, Patrick O. Moore, Paul M. McIntire, editors., American Society for Nondestructive Testing, Inc., (1996).
(4) ASM Handbook, vol. 17, Nondestructive Evaluation and Quality Control, ASM International, p. 231 (1992).
(5) D.K. Hsu, P.K. Liaw, N. Yu, V. Saini, N. Miriyala, L.L. Snead, R.A. Lowden, and C.J. McHargue, Mat. Res. Soc. Symp. Proc., 365, p. 203 (1995).
(6) P.K. Liaw, N. Yu, D.K. Hsu, N. Miriyala, V. Saini, L.L. Snead, C.J. Mchargue, and R.A. Lowden, Journal of Nuclear Materials, 219, p. 93 (1995).
(7) D.C. Kunerth, L.A. Lott, and J.B. Walter, Ceram. Eng. Sci. Proc., 11 (9-11), p. 1685 (1990).
(8) P.K. Liaw, D.K. Hsu, N. Yu, N. Miriyala, V. Saini, and H. Jeong, Acta Metal. et Mater., 44 (5), p. 2101 (1996).
(9) J. Kim and P.K. Liaw, JOM-e, vol. 50, no.11, (1998), (http://www.tms.org/pubs/journals/JOM/9811/Kim/Kim-9811.html).
(10) Nondestructive Testing Handbook, 2nd ed., vol. 10, Nondestructive Testing Overview, S. Ness, and C. N. Sherlock, Technical eds., P. O. Moore and P. M. McIntire, eds., (American Society for Nondestructive Testing, Inc., (1996).
(11) S. Ahuja, W.A. Ellingson, J.S. Steckenrider, and S.J. Koch, Thermal and Mechanical Test Methods and Behavior of Continuous-Fiber Ceramic Composites, ASTM STP 1309, M.G. Jenkins, S.T. Gonczy, E. Lara-Curzio, N.E. Ashbaugh, and L.P. Zawada, Eds., American Society for Testing and Materials, (1997).
(12) H. Wang, R.B. Dinwiddie and P.S. Gaal, Thermal Conductivity, 23, p. 119 (1996).
(13) W.J. Parker, R.J. Jenkins, C.P. Butler, and G.L. Abbott, Journal of Applied Physics, vol. 32 (9), p. 1679 (1961).